

Artificial Neural Network-Controlled Resonant Converter for LED Applications

Prof. Dattatraya Raghoji¹, Prof. Sujatha Kumari², Prof. Kirankumar³

^{1,2,3} Dept. Electrical and Electronics Engineering Shetty Institute of Technology Kalaburgi, Karnataka, India

Abstract—As a result of this research, a high-power-factor resonant LED driver under ANN control is proposed. Both the ANN and the buck power factor correction (PFC) unit rely on a single active switch, which is controlled by the ANN. Output current ripples are minimized by relying on a bulk capacitor and a quick voltage mode control loop in this setup. In spite of a little voltage ripple in pre-stage output bulk capacitor, the duty cycle of the active switch seems to be constant for the half-line cycle. Because the power factor improves when conduction mode is broken, Buck PFCs may be used in this context. The resonance between the resonant capacitor as well as the transformer's leaky inductor causes diodes in a resonance-based dc-dc unit to switch off at zero current. In each LED string, the output current can be balanced by balancing the charge in the resonant capacitor. Thus, the efficiency can be improved. The digital control is replaced by ANN control for improving the transient performance of the projected system. The proposed system is simulated in MATLAB/Simulink software.

Index Terms—LED driver, Flicker-free, ANN, current balancing, power factor correction (PFC).

I. INTRODUCTION

There has been a shift away from incandescent bulbs to higher brightness light-emitting diode (HB LED) bulbs because of their excellent efficiency, rapid response time, broad color range, and long lifespan [1]-[3]. The luminance of the LED is in direct proportion with the forward current of the LED. A single LED's forward voltage and current are constrained by its packaging. The most straightforward technique to create an LED string with the necessary brightness and uniformity is to link many LEDs in series. [4] IEC61000-3-2 Class C standard specifies strict criteria for the harmonic components of power converters in lighting equipment. Harmonics in the input signal may be

effectively muted using power factor correction (PFC). Since the LED driver needs a sinusoidal input current, a PFC unit is necessary for it. In terms of phases, there are three kinds of PFC converters: single-stage, 2-stage, and integrated. Singular-stage and two-stage PFC converters are the simplest to construct.

It's possible to accomplish PFC with output current regulation with the use of a single-stage PFC converter [5]-[6]. A single-stage PFC converter provides outstanding efficiency, cheap cost, and ease of control for the power provided to the output. There will be twice as much line-frequency ripple owing to an abrupt imbalance of power among ac input and output sides. LED flicker is generated by an output ripple that is hazardous to human health. Transient energy imbalance is buffered and low ripple output is achieved using a two-stage [7] LED driver with a PFC converter. Power factor correction (PFC) device in the pre-stage (PF). The output ripple is removed and the output current is regulated by the second stage dc-dc unit. The two-stage manufacturing method is more costly than a single-stage one due to the inclusion of additional components and complex control loops. In order to address the issues with both single-stage and two-stage converters, several researchers have recently focused on integrating PFC and DC-DC units into a single active switch. There is some thought being given to including a boost-buck converter [10]. Minimizing voltage ripple across the dc-link capacitor and achieving PFC via pre-stage boost converter are both accomplished by the converter's use of a fast voltage mode control loop. In order to expand the output branch, however, a greater number of dc capacitors & magnetizing inductors are needed, which in turn increases the converter's cost. In an integrated PFC converter, the high PF and easy control provided by DCM operating modes for pre-stage as well as second-stage inductor currents make them attractive.

Network systems based on biological neurons are known as neural network controllers. Artificial neural networks (often referred to as ANNs) are founded on the notion of learning from the data that they are fed. An input layer, a hidden layer, as well as an output layer, are all part of the ANN controller. The ANN controller was fed a set of training data, and it utilized the system's digital control response as its response. ANN controller acquisition in this article is done using Levenberg Margaret Method [11] as it is the most efficient algorithm for guided learning. For non-linear least squares issues, the damped least squares (DLS) method, often known as Levenberg-Marquardt algorithm (LMA or simply LM), is utilized. These challenges are most noticeable in least-squares curve fitting.

II. LITERATURE SURVEY

This study, presents a high-power-factor, passive-current- balancing, single-switch multi-string LED driver. By using a single active switch & dc link capacitor, it combines a boost PFC converter in the pre-stage with buck dc-dc converters in the second stage [11]. This study proposes a high-power- factor, passive-current-balancing, resonant single-stage, single-switch, four-output LED driver. The four-output LED driver's currents may be individually adjusted using passive current balancing by adjusting the current flowing from a single output. The suggested LED driver simply has one magnetic component and one active switch, making it very cost-effective [6]. With the proposed single-stage isolated

PFC unit functioning in discontinuous conduction mode (DCM) and an isolated DC/DC unit with voltage double rectifier. By using a voltage double rectifier circuit upon that secondary side, the secondary side diodes are protected from excessive power and the isolated transformer may be made much smaller [8]. This article presents a parallel inverted buck converter, which is used to create an ac-dc LED driver. Both power factor correction and energy buffering are both accomplished by a single inverted buck converter that supplies power to a storage capacitor at twice line frequency (PFC). The LEDs' consistent brightness is maintained by the second inverted buck converter, keeping the danger of eye damage from flickering light to a minimum [13]. In order to overcome the flat-spot

issue, this research suggests Levenberg- Marquardt with weight compression (LM-WC), which compresses the weights of individual neurons in order to move the activity away from the saturated zone and toward the linear region [14].

III. THE PROPOSED LED DRIVER

The proposed 3-string LED driver whose structure and control loop is shown in Fig 1. Circuit components include diode- bridge rectifier D_b , filter inductor L_f , filter capacitor C_f , and the buck PFC and resonance DC-DC units. Inductor L_B , freewheel diodes $DB1$, $DB2$, $DB3$, as well as bulk capacitor CB make up the Buck PFC unit. A big capacitance in CB allows for a reduction in voltage ripple under identical input voltage. Because of this, the duty cycle D of $S1$ as well as voltage CB remain practically constant for a half-line cycle. Discontinuous conduction mode may be used with the aforementioned factor with a consistent control loop. To obtain PFC when the inductor current of the L_B is combined. 3 LED string LED_S1 LED_S2 LED_S3 are connected to one of 3 filters capacitors $Co1$, $Co2$, and $Co3$, which in turn are connected to the resonant capacitor C_{r1} and the freewheel diodes $D1$ and $D2$. The transformer T completes the resonant DC-DC circuit. It is possible to compare the transformer into an ideal transformer (which has a turns ratio of n), magnetizing inductor L_m , as well as leaking inductor L_k , respectively. The charge-discharge balancing technique of resonant capacitors is used to provide current balancing among LED strings. Furthermore, the PFC unit, as well as the dc-dc unit, exchanges an active switch $S1$ in order to increase

high power factor AC-DC LED driver, the power switch is shared between a buck-boost efficiency.

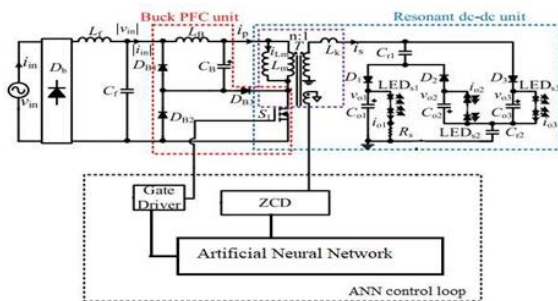


Fig 1. Circuit diagram of Projected LED driver

IV. TRAINING/EXPLANATION OF THE ANN CONTROLLER

In terms of fitting functions, neural networks are excellent. It has been shown that a very basic neural network can be used to do any useful task. There are seven major phases in the design process of neural networks.

1. Data Collection
2. Creating network -Creating Neural Network Object
3. Configuring network — Configuring Neural Network Inputs and Outputs
4. Initializing biases and weights
5. Training network — Training Neural Network Notions
6. Validating network
7. Using network

The Deep Learning Toolbox program stores most of the information needed to model neural networks in network objects. It is necessary to set up and train a neural network once it has been built. Sample data are used to specify how the network should be configured so it becomes consistent with the issue at hand. Adjustable network settings are available after network configuration. (Called biases and weights) and must be tuned to optimize network performance. This process of fine-tuning is known as network training. Example data must be provided to the network during configuration and training. This demonstrates how to format the data for network presentation. Also, it describes network configuration in 2 kinds: incremental training and batch training. To define a fitting issue for the toolbox, arrange Q input vectors in columns into the matrix. Other sets of Q target vectors (each corresponding to a different input) should be organized into a second matrix, as well.

Utilizing Neural Network Fitting App
Launch Neural Network start GUI by this command:
Nnstart

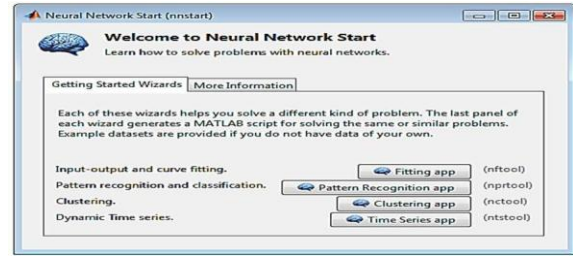


Fig 2. Neural Network start

Click the Fitting app for opening Neural Network Fitting app in a dialogue box that appears as in Fig 3.

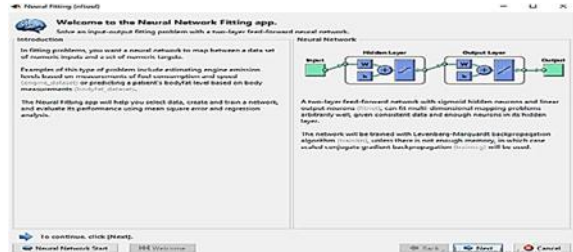


Fig 3. Neural Network fitting app

Click Next to proceed.

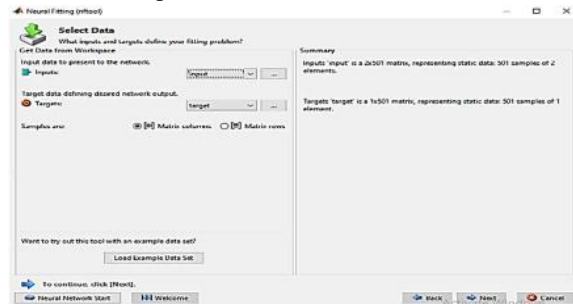


Fig 4. Selection of data

To load data by MATLAB working space, use Target and Input options in the Select Data window as shown in Fig 4.

The validating & Testing Data window, seen in the accompanying image, will appear then on click Next.

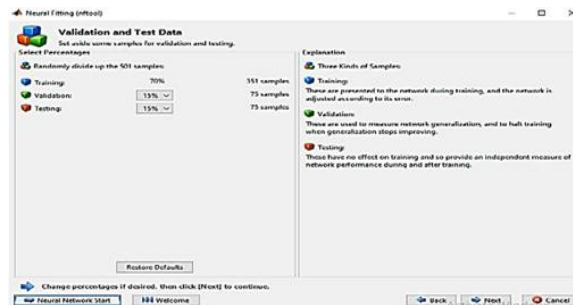


Fig 5. Selection of Training, Validation, and testing percentage

The original data is used for both validation and testing sets, which are all fixed to 15% of it.

As a result of these parameters, three sets of input and target vectors would be generated randomly as shown in Fig 5

- 70% is utilized for training purposes.
- 15% would be utilized for validating the network is general & also must halt training before overfitting.
- The last 15% is utilized like a completely independent network test generalization.

A 2-layer feedforward network is often used for fitting functions, using sigmoid transfer functions in the hidden layer & linear transfer functions in the output layer. By default, the density of hidden neurons is 10. 100 neurons have been shown to be optimal for improving the effectiveness of a network training program.

Then click the Train button to begin training. Bayesian Regularization (trainbr) can require longer but provide a better solution for certain noisy and small situations than Levenberg- Marquardt (trainlm). Scaled Conjugate Gradient (trainscg) is suggested for big issues. Using the usual Levenberg-Marquardt model is the goal of this work.

After six cycles of training, the validation error remained the same (validation stop).

Regression from the Plots menu is used to verify network performance.



Fig 6. Choosing the training algorithm

For a perfect match, data must lie on a 45° line connecting the network's outputs to objectives. The fit is acceptable for every dataset, with R values close to one in each instance. Selecting "retrain" from the nftool menu would allow you to fine-tune your findings even more. It is possible that this may lead to a more effective network after retraining since it will

modify the initial weights and biases of the network significantly.



Fig 7. Evaluation of the network

During this point, you may put the network over its tests using fresh data as shown in Fig 7.

On either original or fresh data, the network's performance may be improved by one of the following options.:

- Training more than once.
- Increasing neuron quantity.
- Increasing training dataset size.

Lowering the amount of neurons may help your results if your training dataset performance is excellent yet your test set efficiency is much lower, which may suggest overfitting. If your training output is subpar, you should consider increasing the number of neurons.

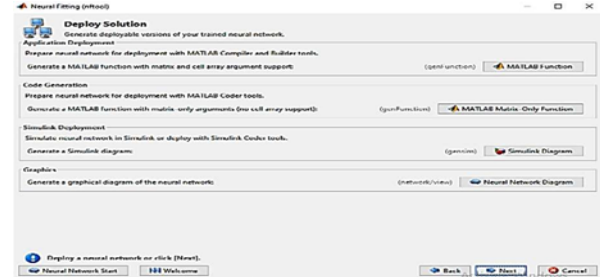


Fig 8. Deploying the solution

MATLAB and Simulink diagrams may be generated using this panel, as can MATLAB functions. There are MATLAB Compiler and other code creation tools available to help you get a better understanding of why neural network interpolates outputs from inputs. To generate the neural network controller block, click the Simulink diagram.

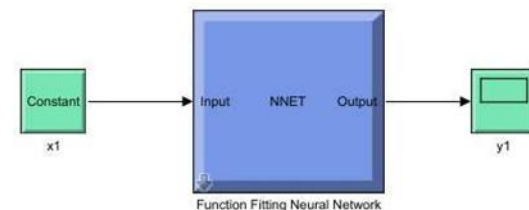


Fig 9. Finalized trained ANN Simulink block

If you train a neural network more than once, the results will vary because each time a new set of weights can be used and biases or divide your data into training, validation, and test groups. Various neural networks trained to solve the same issue may have different results for the same input. Retrain numerous times to guarantee that neural networks with incredible precision have been found. This block as shown in Fig 9 can be attached as a controller to the switch to provide the gate pulses.

V. DESIGN CONSIDERATIONS AND ANALYSIS

Several assumptions are made in order to clarify the design choices and make the analysis simpler:

- 1) Every component used are ideal device.
- 2) When compared to line frequency f_L , switching frequency f_s is substantially higher, resulting in $f_s \gg f_L$.
- 3) Full wave rectified sine wave is used as input voltage., defined as $|V_{in}(t)| = V_p |\sin(\omega L t)|$, here V_p is amplitude & $\omega L = 2\pi f_L$ is angular frequency of the alternating current input voltage.
- 4) Output capacitors (C_{o1} , C_{o2} , C_{o3}) and the bulk capacitor C_B is sufficiently large, the voltage ripple across them could be ignored. While the switching period, the voltage across C_{o1} , C_{o2} , C_{o3} , and C_B could be considered constant.
- 5) The capacitance of resonant capacitors are equal, i.e, $C_{r1} = C_{r2} = C_r$.

A. PRINCIPLE

The rectified line voltage and current are represented by $|V_{in}|$ and $|I_{in}|$, respectively. The voltage across C_B is denoted by V_B . The operation in a half-line cycle is divided into two intervals based on the relationship between $|V_{in}|$ and V_B , that is Interval-I ($|V_{in}| > V_B$) and Interval-II ($|V_{in}| < V_B$).

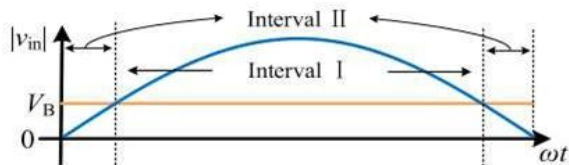


Fig 10. Waveforms of rectified line voltage with bulk capacitor voltage

1) Interval I

While rectified line voltage $|V_{in}|$ is more than V_B , the circuit works into interval I, which has five operation modes.

a) Mode 1:

The switch S_1 is powered on the primary side. Diode DB_2 is conducting while the capacitor C_B discharges due to magnetizing inductance. DB_1 and DB_3 are biased (negative). The supply voltage charges the inductor L_b .

The L_k is in resonance with C_{r1} and C_{r2} on the secondary side. The diodes DB_1 and DB_3 are in forwarding bias (positive) and provide a path for energy into primary induction to be transferred to LED_{s1} and LED_{s3} . Because DB_2 is not conducting, C_{o2} powers LED_{s2} . Mode 2 begins when the capacitor C_B on the primary side is completely discharged.

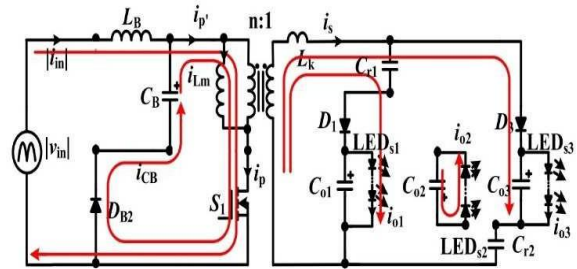


Fig 11. Interval I Mode 1 Equivalent circuit

b) Mode 2:

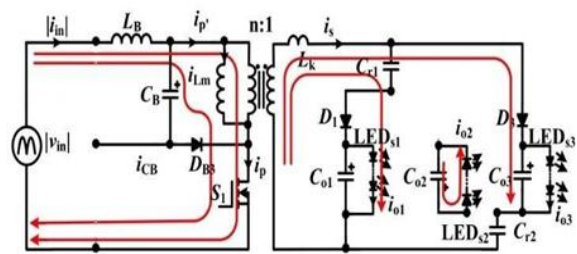


Fig 12. Interval I Mode 2 Equivalent circuit

On the primary side, L_B and C_B are charging as DB_2 enters reverse bias mode and DB_3 begins conducting. On the secondary side, the C_{r1} and C_{r2} continue to discharge until the capacitor current reaches zero and thus the secondary current of the transformer reaches zero.

c) Mode 3:

In this mode, the primary side continues as in mode 2, and capacitors C_{o1} , C_{o2} , and C_{o3} provide energy to the respective LEDs_{s1}, LEDs_{s2}, and LEDs_{s3} on the secondary side.

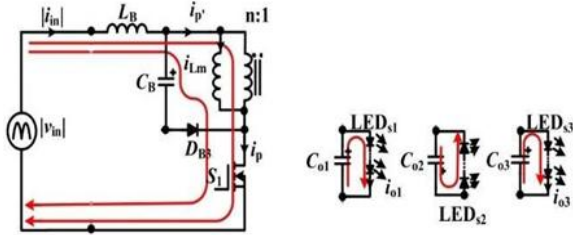


Fig 13. Interval I Mode 3 Equivalent circuit

d) Mode 4:

Primarily, inductor L_B starts discharging and charges capacitor C_B via diode D_{B2} . The power present in magnetized inductance L_M is released via primary winding. Capacitors C_{r1} and C_{r2} begin charging on the secondary side. Mode 5 is activated when the inductor L_B is completely discharged.

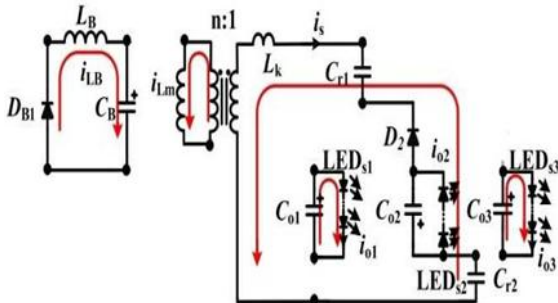


Fig 14. Interval I Mode 4 Equivalent circuit

e) Mode 5:

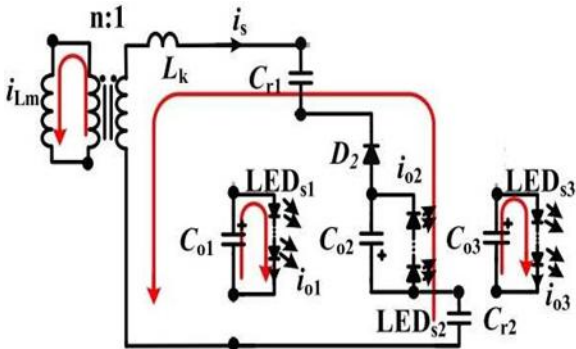


Fig 15. Interval I Mode 5 Equivalent circuit

On the primary side, the L_M continues to discharge its

energy while the capacitors C_{r1} and C_{r2} charge. This mode is terminated when L_M is totally discharged, thus interval I is completed.

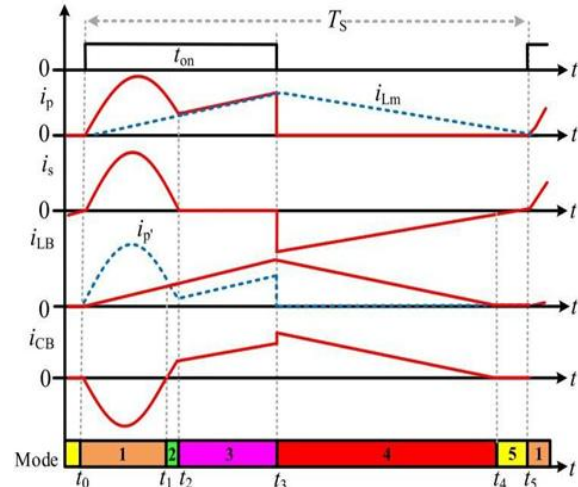


Fig 16. Waveforms for the Interval I

2) Interval II

Whenever rectified line voltage $|V_{in}|$ is less than V_B , the circuit functions in interval II, which has 3 operation methods.

a) Mode 1:

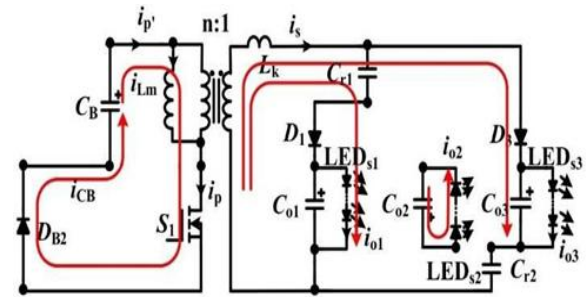


Fig 17. Interval II Mode 1 Equivalent circuit

The operating phase is equivalent as mode 1 into the interval I, with the exception that capacitor C_B delivers separate power for load into mode 1 of interval II, where the supply voltage is lower than V_B and the L_B is neither charging nor discharging. The voltage of the magnetizing inductor L_M rises linear. Whenever secondary current I_s reaches 0, interval II mode 2 begins.

b) Mode 2:

On the primary side, the C_B continues to discharge via primary inductance, while on the secondary side, C_{o1} , C_{o2} , and C_{o3} continue to discharge and supply

the corresponding LEDs₁, LEDs₂, and LEDs₃. When S1 is turned off, the next mode begins.

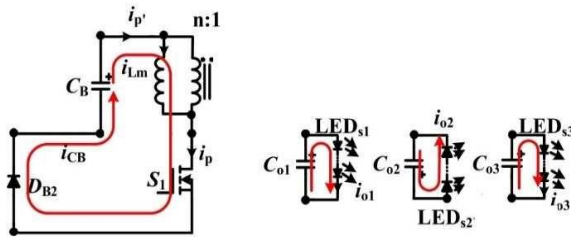


Fig 18. Interval II Mode 2 Equivalent circuit

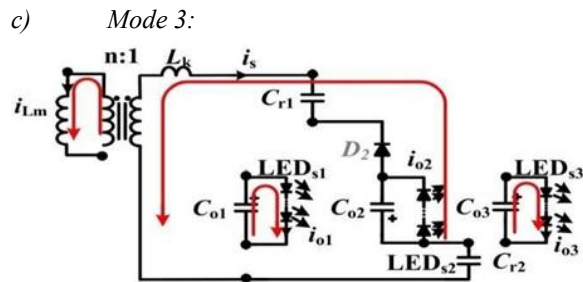


Fig 19. Interval II Mode 3 Equivalent circuit

The L_m begins to discharge on the primary side via primary inductance, while the capacitors C_{r1} and C_{r2} charge on the secondary side. When L_m is fully discharged, a new switching period begins.

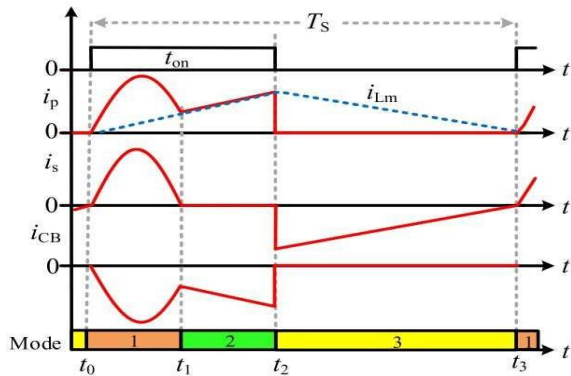


Fig 20. Waveforms for the Interval II

VI. SIMULATION AND ITS RESULTS

The proposed ANN Control-based Resonant LED Driver having Higher Power Factor is being simulated for R load as LED are resistive load with simulating outcomes are contrasted by digital control loop and ANN controller with respect to efficiency and power factor. The resistive load $R = 220\Omega$ and the Fig 22 is the simulation circuits of the proposed LED

driver with a digital controller. The output voltage is varied between 71.1 – 72.5V.

Fig 24 is the simulation circuits of the proposed LED driver with an ANN controller. The output voltage is constant at 72.5V

In the Digital controller and the ANN controller, the input voltage is varied from 260V to 180 V at $t=0.2s$. The digital controller is providing the load voltage regulation in order to maintain the light intensity of the LEDs. The load voltage and current of an LED driver with the digital controller is provided below in Fig 23.

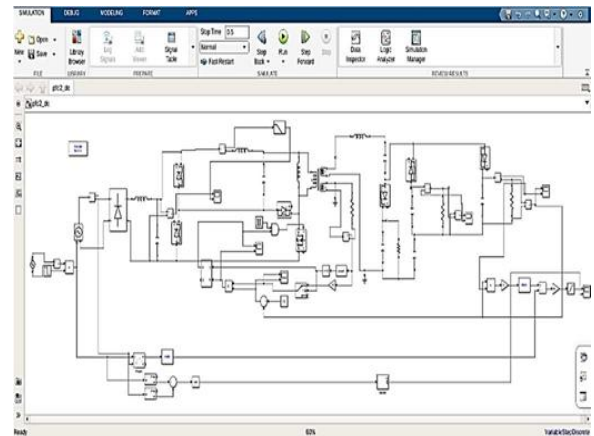


Fig 21. Simulation circuit of the proposed LED driver with a digital controller

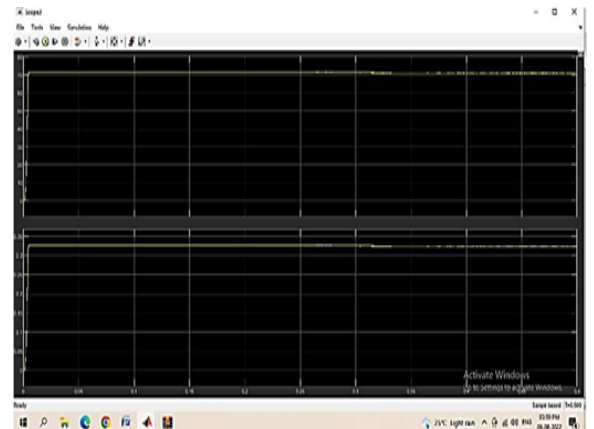


Fig 22. Load voltage and current of led driver circuit with digital controller

The load voltage reduced from 72V to 71.1V with the change in the input voltage from 260V to 180V. The required %regulation is around 1.25%. The simulation circuit for the LED driver circuit with ANN controller is provided below in Fig 24

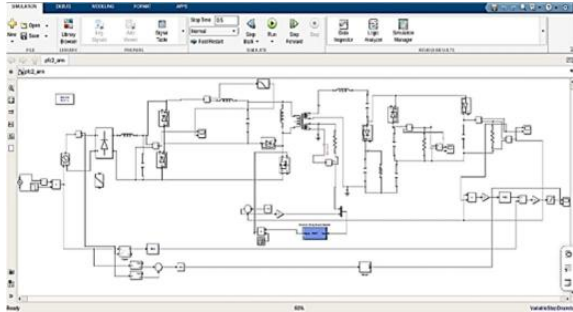


Fig 23. Simulation circuit of the proposed LED driver with an ANN controller

In this, the ANN controller replaces the digital controller in order to improve the performance of the LED driver circuit. The load voltage and current for the LED driver circuit with ANN controller is provided below in Fig 25

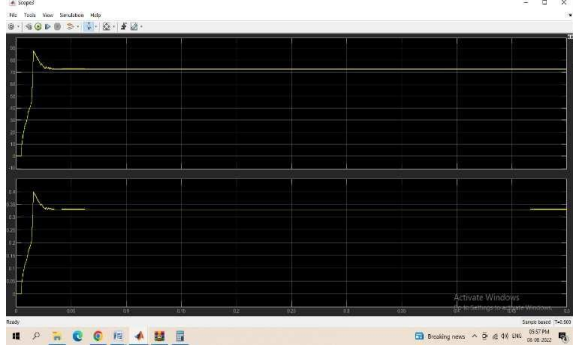


Fig 24. Load voltage and current of led driver circuit with ANN controller

The load voltage is maintained at 72.5V with the change in the input voltage of 260V to 180V. The required %regulation is around -0.69%.

The efficiency & power factor of the LED driver circuit is measured with digital and ANN controller and provided below in Fig 26 and 27 respectively.

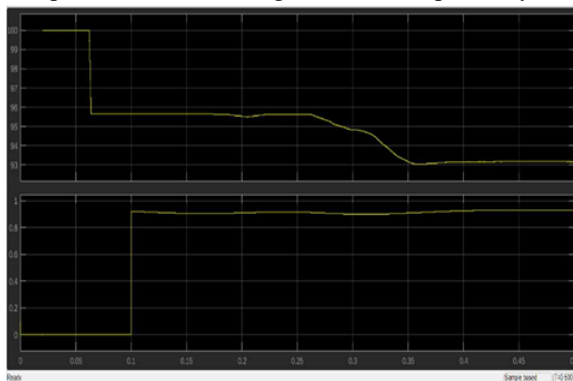


Fig 25. Fig 25: Efficiency and Power factor of Digital controller

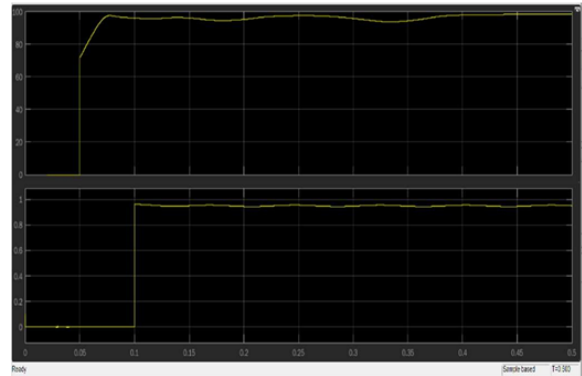


Fig 26. Efficiency and Power factor of ANN controller

Above are the simulation results of the digital controller and ANN controller are provided and a brief comparison is made on the Power factor and Efficiency.

Simulated outcomes portray that the efficiency and power factor of the digital control is around 92% and 0.94 and whereas the power factor and efficiency of the ANN controller are around 98% and 0.955 for an output restive load of 220Ω.

Parameters	Digital Controller	ANN Controller
Load Voltage	72V – 71.1V	72.5V
% Regulation	1.25%	0.69%
Efficiency	92%	98%
Power Factor	0.94	0.955

Table1. Comparisons of Digital and ANN Controller

VII. CONCLUSION

This study proposes an ANN Controlled Resonant LED Driver having a High-Power Factor. The suggested ANN Controlled LED driver merges a buck PFC and a resonant dc-dc unit while disseminating a singular active switch. The charge balance of 2 resonant capacitors may be used to automatically balance the output current of every LED string. An ANN controller is trained using target data and inputs from the digital controller's input and outputs. Simulated outcomes were contrasted among digital and neural network control using MATLAB/Simulink

software. The proposed driver has an efficiency of 92 percent, 0.94 Power Factor when using a digital controller, and

an efficiency of 98 percent, 0.95 Power Factor when using an ANN controller. As a result, it is concluded that the ANN controller produces better and more accurate results than the digital controller.

REFERENCES

- [1] X. Qu, S. C. Wong, and K. T. Chi, "Noncascading structure for electronic ballast design for multiple LED lamps with independent brightness control," *IEEE Trans. Power Electron.*, vol. 25, no. 2, pp. 331–340, Mar. 2010.
- [2] M. Meraj, S. Rahman, A. Iqbal, and L. Ben-Brahim, "High brightness and high voltage dimmable LED driver for an advanced lighting system," *IEEE Access*, vol. 7, pp. 95643–95652, 2019.
- [3] X. Liu, X. Li, Q. Zhou, and J. Xu, "Flicker-free single switch multi- string LED driver with high power factor and current balancing," *IEEE Trans. Power Electron.*, vol. 34, no. 7, pp. 6747–6759, Jul. 2019.
- [4] Magnetic Compatibility (EMC), Part 3-2: Limits-Limits for Harmonic Current Emissions (Equipment Current ≤ 16 A Per Phase), International Standard IEC 61000-3-2, 2009.
- [5] J. Lee, J.-M. Kwon, E.-H. Kim, W.-Y. Choi, and B.-H. Kwon, "Single- stage single-switch PFC flyback converter using a synchronous rectifier," *IEEE Trans. Ind. Electron.*, vol. 55, no. 3, pp. 1352–1365, Mar. 2008.
- [6] X. Liu, Q. Yang, Q. Zhou, J. Xu, and G. Zhou, "Single-stage single- switch four-output resonant LED driver with high power factor and passive current balancing," *IEEE Trans. Power Electron.*, vol. 32, no. 6, pp. 4566–4576, Jun. 2017.
- [7] Y.-S. Lai and Z.-J. Su, "New integrated control technique for two-stage server power to improve efficiency under the light-load condition," *IEEE Trans. Ind. Electron.*, vol. 62, no. 11, pp. 6944–6954, Nov. 2015.
- [8] Q. Luo, J. Huang, Q. He, K. Ma, and L. Zhou, "Analysis and design of a single-stage isolated AC–DC LED driver with a voltage doubler rectifier," *IEEE Trans. Ind. Electron.*, vol. 64, no. 7, pp. 5807–5817, Jul. 2017.
- [9] Z. Nie and A. Emadi, "Buck integrated forward converter," in *Proc. IEEE 36th Conf. Power Electron. Spec.*, Jun. 2005, pp. 1446–1451.
- [10] X. Liu, X. Li, Q. Zhou, and J. Xu, "Flicker-free single switch multi- string LED driver with high power factor and current balancing," *IEEE Trans. Power Electron.*, vol. 34, no. 7, pp. 6747–6759, Jul. 2019.
- [11] I. Yang and K. Kim, "Development of artificial neural network model for the prediction of descending time of room air temperature", *Int. J. Air-Cond. Refrig.*, vol. 12, pp. 1038-1048, 2000.
- [12] Hyun-Chang Kim, Moon Chul Choi, Sungwoo Kim, and Deog-Kyoon Jeong, "An AC–DC LED driver with a two-parallel inverted buck topology for reducing the light flicker in lighting applications to low- risk levels," *IEEE Trans. Power Electron.*, vol. 32, no. 5, pp. 3879-3891, May. 2017.
- [13] James S. Smith; Bo Wu; Bogdan M. Wilamowski, "Neural Network Training with Levenberg-Marquart and adaptable weight compression", *IEEE Transactions on Neural Networks and Learning Systems Volume: 30, Issue: 2, February 2019.*
- [14] Shufang Zhang; He Huang; Ziyang Han, "A Levenberg-Marquardt Algorithm Based Incremental Scheme for Complex-Valued Neural Networks", *2019 IEEE Symposium Series on Computational Intelligence (SSCI).*